

# Narrow Band Gap D–A Copolymer of Indacenodithiophene and Diketopyrrolopyrrole with Deep HOMO Level: Synthesis and Application in Field-Effect Transistors and Polymer Solar Cells

Xiaochen Wang,<sup>1</sup> Hao Luo,<sup>2</sup> Yeping Sun,<sup>1,2</sup> Maojie Zhang,<sup>2</sup> Xiaoyu Li,<sup>1</sup> Gui Yu,<sup>2</sup> Yunqi Liu,<sup>2</sup> Yongfang Li,<sup>2</sup> Haiqiao Wang<sup>1</sup>

<sup>1</sup>Key Laboratory of Carbon Fiber and Functional Polymers, Ministry of Education, College of Materials Science and Engineering, Beijing University of Chemical Technology, Beijing 100029, People's Republic of China

<sup>2</sup>Beijing National Laboratory for Molecular Sciences, CAS Key Laboratory of Organic Solids, Institute of Chemistry, Chinese Academy of Sciences, Beijing 100190, People's Republic of China

Correspondence to: H. Wang (E-mail: wanghaiqiao@mail.buct.edu.cn), X. Li (E-mail: lixy@mail.buct.edu.cn), Y. Li (E-mail: liyf@iccas.ac.cn), or G. Yu (E-mail: yug@iccas.ac.cn)

Received 24 August 2011; accepted 3 October 2011; published online 31 October 2011

DOI: 10.1002/pola.25042

**ABSTRACT:** A novel fused ladder alternating D–A copolymer, PIDT–DPP, with alkyl substituted indacenodithiophene (IDT) as donor unit and diketopyrrolopyrrole (DPP) as acceptor unit, was designed and synthesized by Pd-catalyzed Stille-coupling method. The copolymer showed good solubility and film-forming ability combining with good thermal stability. PIDT–DPP exhibited a broad absorption band from 350 to 900 nm with an absorption peak centered at 735 nm. The optical band gap determined from the onset of absorption of the polymer film was 1.37 eV. The highest occupied molecular orbital level of the polymer is as deep as –5.32 eV. The solution-processed organic field-effect transistor (OFETs) was fabricated with bottom gate/top

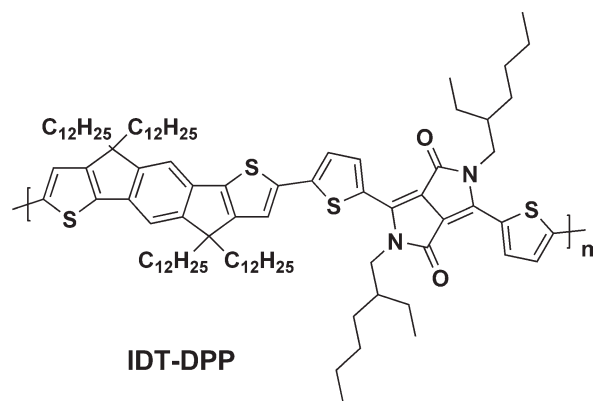
contact geometry. The highest FET hole mobility of PIDT–DPP reached  $0.065 \text{ cm}^2 \text{ V}^{-1} \text{ s}^{-1}$  with an on/off ratio of  $4.6 \times 10^5$ . This mobility is one of the highest values for narrow band gap conjugated polymers. The power conversion efficiency of the polymer solar cell based on the polymer as donor was 1.76% with a high open circuit voltage of 0.88 V. To the best of our knowledge, this is the first report on the photovoltaic properties of alkyl substituted IDT-based polymers. © 2011 Wiley Periodicals, Inc. *J Polym Sci Part A: Polym Chem* 50: 371–377, 2012

**KEYWORDS:** conjugated polymers; diketopyrrolopyrrole; indacenodithiophene; organic field-effect transistors; polymer solar cells

**INTRODUCTION** During the last decade, conjugated polymer materials have been the focus of both scientific research and industry, because of their excellent electronic and optoelectronic properties. Up to now, conjugated polymers have been successfully used in many optoelectronic devices, such as organic light emitting diodes, organic field-effect transistors (OFETs), polymer solar cells (PSCs), and so on.<sup>1–10</sup> Recently, indacenodithiophene (IDT) containing polymers have attracted much attention because the fused ring unit in IDT can enhance both the coplanarity of the molecular backbones and the  $\pi$ – $\pi$  stacking in the solid state of polymers and consequently qualify these kinds of polymers as particularly promising candidates for applications in PSCs and OFETs. The copolymers based on tetraalkyl substituted IDT unit showed hole mobilities as high as  $1 \text{ cm}^2 \text{ V}^{-1} \text{ s}^{-1}$ .<sup>11</sup> Some of the tetraphenyl substituted IDT-based polymers were also investigated in PSCs. Although the PSCs based on tetraphenyl substituted IDT polymers exhibited power conversion efficiency (PCE) of 2.0–6.41%,<sup>12–15</sup> the hole mobility of these

polymers are much lower ( $10^{-9}$ – $10^{-3} \text{ cm}^2 \text{ V}^{-1} \text{ s}^{-1}$ ) than that of alkyl substituted IDT-based polymers. This is because the phenyl rings in the IDT unit could induce steric hindrance to interrupt coplanarity of polymer backbones and intermolecular stacking between polymer chains. From this point of view, tetraalkyl substituted IDT-based copolymers would facilitate high performance of PSCs and OFETs.

Despite a large number of reports on copolymers based on tetraphenyl substituted IDT, there have been very few studies on the syntheses of the alkyl substituted IDT copolymers and the applications in the PSCs and OFETs. Here, we designed and synthesized a novel fused ladder alternating D–A copolymer, PIDT–DPP, with alkyl substituted IDT as donor unit and diketopyrrolopyrrole (DPP) as acceptor unit. The structure of PIDT–DPP is shown in Scheme 1. In PIDT–DPP, the IDT unit was used to enhance both the coplanarity of the molecular backbone and the  $\pi$ – $\pi$  stacking in the solid state of the copolymer, whereas the electron deficient nature of DPP unit was



**SCHEME 1** Molecular structure of the PIDT-DPP.

used to construct donor–acceptor structure with narrow band gap, which would facilitate high performance of PSCs or OFETs.<sup>16–19</sup> In addition, the well-defined alternating D–A structure of polymer combined with the linear alkyl side chains is expected to optimize the molecular packing in the solid state. In this article, OFETs and PSCs based on the polymer were fabricated and characterized. The highest FET hole mobility of PIDT-DPP reached  $0.065 \text{ cm}^2 \text{ V}^{-1} \text{ s}^{-1}$  with an on/off ratio of  $4.6 \times 10^5$ . The PCE of the PSCs was 1.76%, under the illumination of AM 1.5 and  $100 \text{ mW/cm}^2$ , with a broad photoresponse spectrum covering from 300 to 900 nm. To the best of our knowledge, this is the first report on the photovoltaic properties of alkyl substituted IDT-based polymer.

## EXPERIMENTAL

### Materials

3,6-Bis(5-bromothiophen-2-yl)-2,5-bis(2-ethylhexyl)pyrrolo[3,4-c]pyrrole-1,4(2H,5H)-dione, (DPP), was synthesized as reported in the literature.<sup>20</sup> Tetrahydrofuran (THF) was dried over Na/benzophenone ketyl and freshly distilled before use. Other reagents and solvents were commercial grade and used as received without further purification. All reactions were performed under nitrogen atmosphere.

### Measurements and Characterization

The molecular weight of the polymer was measured by gel permeation chromatography (GPC) method. The GPC measurements were performed on Waters 515-2410 with polystyrenes as reference standard and THF as an eluent. All new compounds were characterized by nuclear magnetic resonance (NMR) spectra. The NMRs were recorded on a Bruker AV 600 spectrometer in  $\text{CDCl}_3$  or DMSO at room temperature. Chemical shifts of  $^1\text{H}$  NMR were reported in ppm. Splitting patterns were designated as s (singlet), t (triplet), d (doublet), m (multiplet), and br (broaden). Elemental analyses were performed on a Flash EA 1112 analyzer or Elementar vario EL III. Thermal gravimetric analysis (TGA, Netzsch TG209C) and the differential scanning calorimetry (DSC, TA-Q100) measurements were performed under a nitrogen atmosphere at a heating rate of  $10 \text{ }^\circ\text{C/min}$ . UV-Vis absorption spectra were recorded on a Shimadzu spectrometer

model UV-3150. Absorption spectra measurements of the polymer solutions were performed in chloroform (analytical reagent) at  $25 \text{ }^\circ\text{C}$ . Absorption spectra measurements of the polymer films were performed on the quartz plates with the polymer films spin-coated from the polymer solutions in chloroform (analytical reagent) at  $25 \text{ }^\circ\text{C}$ . The electrochemical cyclic voltammetry was conducted on a Zahner IM6e electrochemical workstation with a Pt plate, Pt wire, and  $\text{Ag/Ag}^+$  electrode as the working electrode, counter electrode, and reference electrode, respectively, in a  $0.1 \text{ mol/L}$  tetrabutylammonium hexafluorophosphate ( $\text{Bu}_4\text{NPF}_6$ ) acetonitrile solution. Polymer thin films were formed by drop casting  $1.0 \text{ mm}^3$  of polymer solutions in THF (analytical reagent,  $1 \text{ mg/mL}$ ) on the working electrode and then drying in air.

### Fabrication of Field-Effect Transistor Devices

Thin-film OFETs were fabricated on highly doped silicon substrates with thermally grown 300-nm-thick silicon oxide ( $\text{SiO}_2$ ) insulating layer, where the substrate served as a common gate electrode. Before polymer semiconductor deposition, the substrates were treated with the silylating agent octyltrichlorosilane (OTS). Thin semiconductor films were then deposited by spin-coating the polymer solutions in  $\text{CHCl}_3$  on the substrates. The film thickness was measured by an XP-2 surface profilometer (Ambios Technology). The samples were then dried and annealed at  $80\text{--}100 \text{ }^\circ\text{C}$  under nitrogen. Source and drain gold electrodes of transistor were vacuum deposited on the polymer layer to form top-contact geometry. Then, the Au electrode was deposited on the polymer layer by vacuum evaporation under  $7 \times 10^{-4} \text{ Pa}$ . The electrical characterization of the transistor devices was performed using a Keithley 4200 semiconductor parameter analyzer.

### Fabrication of Photovoltaic Devices

PSCs were fabricated with indium tin oxide (ITO) glass as a positive electrode, Ca/Al as a negative electrode, and the blend film of the polymer/PCBM between them as a photosensitive layer. The ITO glass was precleaned and modified by a thin layer of poly(3,4-ethylene dioxithiophene):poly(styrene sulfonate) (PEDOT:PSS), which was spin-cast from a PEDOT:PSS aqueous solution (Clevious P VP AI 4083 H. C. Stark, Germany) on the ITO substrate and the thickness of the PEDOT:PSS layer was about 60 nm. The photosensitive layer was prepared by spin-coating a blend solution of the polymer and  $\text{PC}_{70}\text{BM}$  with a weight ratio of 1:1 in *o*-dichlorobenzene at 1500 rpm on the ITO/PEDOT:PSS electrode. Then, the Ca/Al cathode was deposited on the polymer layer by vacuum evaporation under  $3 \times 10^{-4} \text{ Pa}$ . The thickness of the photosensitive layer was about 60 nm, measured on an Ambios Tech XP-2 profilometer. The effective area of one cell was about  $4 \text{ mm}^2$ . The current–voltage ( $I$  vs.  $V$ ) measurement of the devices was conducted on a computer controlled Keithley 236 source measure unit. A xenon lamp with an AM 1.5 filter was used as the white-light source and the optical power at the sample was  $100 \text{ mW/cm}^2$ .

### Synthesis of the Monomers

#### 2,5-Dithien-2-yl-terephthalic Acid Diethyl Ester (1)

To a mixture of diethyl 2,5-dibromoterephthalate (16.7 g, 44 mmol), 2-thiophenylboric acid (12.8 g, 100 mmol) in 300 mL

THF, NaHCO<sub>3</sub> (21 g, 250 mmol) and 100 mL H<sub>2</sub>O were added. The solution was flushed with nitrogen for 10 min and then Pd(PPh<sub>3</sub>)<sub>4</sub> (0.6 g, 0.5 mmol) was added. After another flushing with nitrogen for 20 min, the reactant was heated to reflux for 48 h. After cooled to room temperature, the reaction mixture was poured into saturated NH<sub>4</sub>Cl solution. The product was extracted with ethyl acetate (3 × 150 mL). The extracts were combined and washed with water and brine then dried over Na<sub>2</sub>SO<sub>4</sub>. After filtration, the solvent was removed under reduced pressure. The residue was purified by column chromatography on silica, eluting with petroleum ether/ethyl acetate (from 20:0 to 20:1), to give 2,5-dithien-2-ylterephthalic acid diethyl ester as white crystal (15 g, 88%). <sup>1</sup>H NMR (600 MHz, CDCl<sub>3</sub>, ppm): δ 7.82 (s, 2H, Ar-H), 7.41 (dd, 2H, Ar-H), 7.08–7.10 (m, 4H, Ar-H), 4.22 (q, 4H, CH<sub>2</sub>), 1.16 (t, 6H, CH<sub>3</sub>).

#### 2,5-Dithien-2-yl-terephthalic acid (2)

To a solution of compound 1 (13.5 g, 35 mmol) in ethanol (500 mL), a solution of sodium hydroxide (16 g NaOH in 120 mL water) was added. This mixture was heated at reflux over night. After cooled to room temperature, the solvent was removed under reduced pressure. Then, the residue was added to concentrated hydrochloric acid. The precipitate was collected by filtration and washed with water then dried *in vacuo* to afford product as off-white solid (9.1 g, 79%). <sup>1</sup>H NMR (600 MHz, DMSO-*d*<sub>6</sub>, ppm): δ 13.43 (s, 2H, COOH), 7.69 (s, 2H, Ar-H), 7.67 (dd, 2H, Ar-H), 7.26 (m, 2H, Ar-H), 7.15 (m, 2H, Ar-H).

#### 4,9-Dihydro-s-indaceno[1,2-b:5,6-b']-dithiophene-4,9-dione (4)

To a suspension of compound 2 (6.6 g, 20 mmol) in anhydrous DCM (200 mL, containing 1 mL DMF), a solution of oxalyl chloride (10.2 g, 80 mmol) in 100 mL DCM was added dropwise at room temperature. The mixture was stirred overnight. The solvent was removed under reduced pressure to afford crude acid dichloride as a yellow solid. The residue was redissolved in anhydrous DCM (150 mL) and then added to a suspension of anhydrous AlCl<sub>3</sub> (13 g) in DCM (300 mL) at 0 °C. The resultant mixture was allowed to warm to room temperature and stirred overnight and then poured into cold 2 M hydrochloric acid. The precipitate was collected by filtration and washed with diluted hydrochloric acid, water, and acetone and then dried *in vacuo* to afford a deep blue solid (5.17 g, 86%). MS(*m/z*): 294 (M<sup>+</sup>, 100%), 281, 266, 207, 193; IR (KBr, thin film, cm<sup>-1</sup>) 1706 (C=O).

#### 4,9-Dihydro-s-indaceno[1,2-b:5,6-b']-dithiophene (5)

A mixture of compound 4 (7.35 g, 25 mmol), hydrazine monohydrate (25 g, 0.5 mol) and KOH (28 g, 0.5 mol) in diethylene glycol (250 mL) was heated at 180 °C for 24 h and then poured into cold 2 M hydrochloric acid. The precipitate was collected by filtration and washed with water and acetone, and dried *in vacuo* to give 4,9-dihydro-s-indaceno[1,2-b:5,6-b']-dithiophene as a brown solid (5.2 g, 78%). <sup>1</sup>H NMR (600 MHz, DMSO-*d*<sub>6</sub>, ppm): δ 7.71 (s, 2H, Ar-H), 7.54 (d, *J* = 4.8 Hz, 2H, Ar-H), 7.20 (d, *J* = 4.8 Hz, 2H, Ar-H), 3.78 (s, 4H, CH<sub>2</sub>).

#### 4,9-Dihydro-4,4,9,9-tetrahexadecyl-s-indaceno[1,2-b:5,6-b']-dithiophene (6)

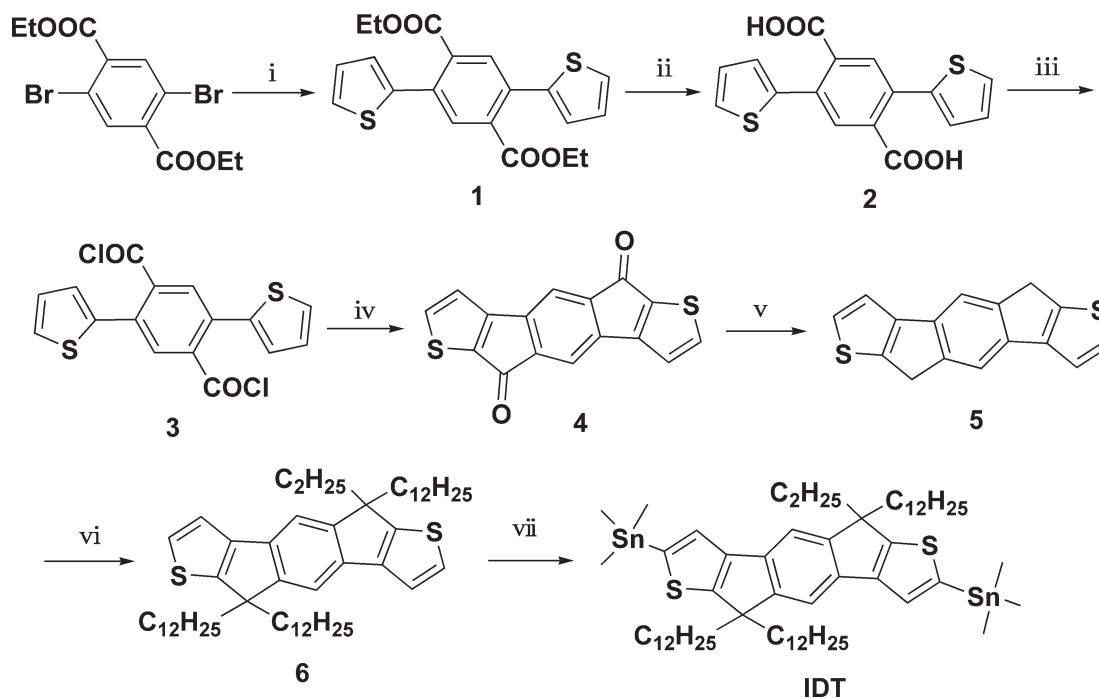
KOH (6.72 g, 0.12 mol) and KI (0.5 g, 3 mmol) were added to a suspension of compound 5 (3.19 g, 12 mmol) in anhydrous DMSO (100 mL). The reaction mixture was stirred for 1 h, followed by the dropwise addition of 1-bromododecane (18.5 g, 74 mmol). Then, the mixture was heated at 80 °C over night. CHCl<sub>3</sub> (200 mL) was added when the mixture cooled to about 50 °C. The mixture was stirred for another 1 h and then poured into cold water. The CHCl<sub>3</sub> phase was separated and concentrated. The residue was purified by column chromatography on silica, eluting with petroleum ether, to give a light yellow crystal (9 g, 80%). <sup>1</sup>H NMR (600 MHz, CDCl<sub>3</sub>, ppm) δ 7.27 (s, 2H, Ar-H), 7.25 (d, *J* = 4.8 Hz, 2H, Ar-H), 6.96 (d, 2H, Ar-H), 1.97–1.96 (m, 4H, CH<sub>2</sub>), 1.85–1.84 (m, 4H, CH<sub>2</sub>), 1.28 (m, 8H, CH<sub>2</sub>), 1.25–1.13 (m, 48H, CH<sub>2</sub>), 1.09 (m, 24H, CH<sub>2</sub>), 0.87 (m, 12H, CH<sub>3</sub>).

#### 2,7-Bis(trimethyltin)-4,9-dihydro-4,4,9,9-tetradodecyl-s-indaceno[1,2-b:5,6-b']-dithiophene

Compound 6 (2.83 g, 3 mmol) was dissolved in dry THF (100 mL). The solution was cooled to -78 °C and butyllithium (2.5 M, 3 mL, 7.5 mmol) was added dropwise over 10 min. The reaction mixture was stirred at this temperature for 1 h. Trimethyltin chloride (1 M in hexanes, 9.0 mL, 9.0 mmol) was added dropwise. The reaction mixture was allowed to warm to room temperature and stirred overnight. Water was added, and the reaction mixture was extracted with diethyl ether. The organic layer was washed with water and dried over magnesium sulfate. Evaporation of the solvent afforded the bis(trimethyltin) monomer as a light brownish viscous oil (3.5 g, 92%). <sup>1</sup>H NMR (400 MHz, CDCl<sub>3</sub>, ppm) δ 7.17 (s, 2H, Ar-H), 6.97 (s, 2H, Ar-H), 1.91–1.95 (m, 4H, CH<sub>2</sub>), 1.81–1.84 (m, 4H, CH<sub>2</sub>), 1.00–1.53 (m, 88H, CH<sub>2</sub>), 0.84–0.87 (m, 30H, CH<sub>2</sub> and CH<sub>3</sub>).

#### Synthesis of the Polymer

IDT monomer (259 mg, 0.2 mmol) and DPP monomer (136 mg, 0.2 mmol) were put into a 25-mL two-neck flask and then 6 mL of chlorobenzene was added. The mixture was stirred and purged with argon for 10 min and then Pd<sub>2</sub>(dba)<sub>3</sub> (10 mg, 0.01 mmol) and (*o*-tol)<sub>3</sub>P (25 mg, 0.08 mmol) were added. After being purged for 15 min, the mixture was heated at 140 °C for 72 h. After cooled to room temperature, the reaction mixture was added dropwise to 200 mL acidic methanol (HCl + CH<sub>3</sub>OH) and then collected by filtration and washed with methanol. The black solid was filtered into a Soxhlet funnel and extracted by methanol, ether, and chloroform successively. The polymer recovered from chloroform was purified by preparative GPC. Then, the product was dried under vacuum for 1 day to recover the target polymer PIDT-DPP as a black solid. (Yield 76%, *M*<sub>n</sub> = 20.8 kDa, *M*<sub>w</sub> = 50.0 kDa, PDI = 2.4.) <sup>1</sup>H NMR (600 MHz, CDCl<sub>3</sub>, ppm) 8.97 (m, 2H), 7.45 (br, 2H), 7.36 (br, 2H), 7.22 (m, 2H), 4.10 (br, 4H), 2.00 (br, 4H), 1.91 (br, 4H), 1.54 (br, 8H), 1.43 (br, 8H), 1.33–1.13 (br, 50H), 0.96–0.92 (br, 32H), 0.84 (br, 24H). Anal. Calcd for (C<sub>94</sub>H<sub>142</sub>N<sub>2</sub>O<sub>2</sub>S<sub>4</sub>)<sub>*n*</sub>: C, 77.24; H, 9.72; N, 1.92. Found: C, 77.31; H, 9.73; N, 2.00.



**SCHEME 2** Synthetic routes of the monomers. (i) 2-Thiophenylboric acid, Pd(PPh<sub>3</sub>)<sub>4</sub>, THF, NaHCO<sub>3</sub>, H<sub>2</sub>O, reflux; (ii) NaOH, H<sub>2</sub>O, reflux and then concentrated hydrochloric acid; (iii) oxalyl chloride, DCM, DMF, room temperature; (iv) AlCl<sub>3</sub>, DCM, 0 °C to room temperature; (v) hydrazine monohydrate, KOH, diethylene glycol, 180 °C; (vi) bromododecane, KOH, KI, DMSO, 80 °C; and (vii) *n*-BuLi, THF, –78 °C to room temperature and then trimethyltin chloride, –78 °C to room temperature.

## RESULTS AND DISCUSSION

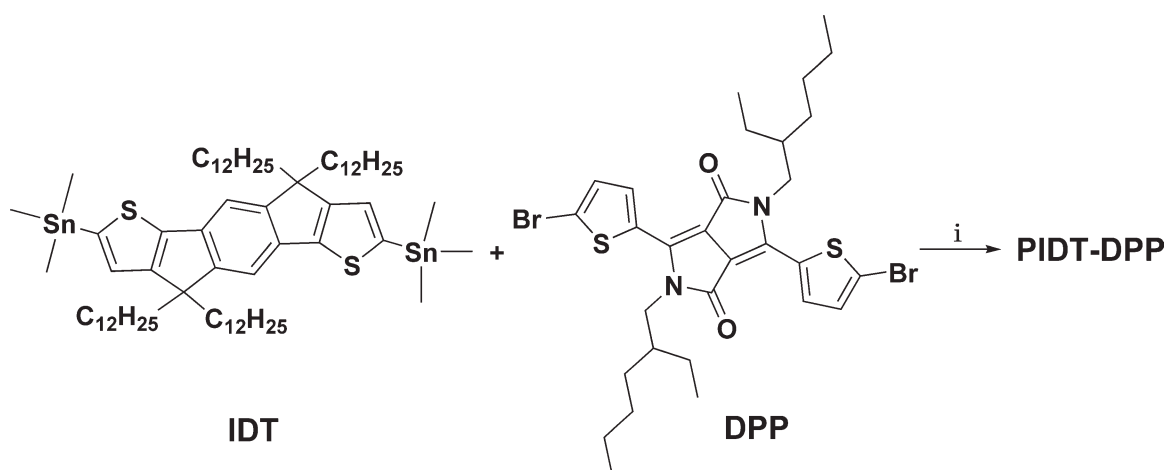
### Synthesis of Monomers and Polymer

The synthetic routes of monomers and corresponding polymer are outlined in Schemes 2 and 3, respectively. The synthesis of the polymer was performed using palladium-catalyzed Stille-coupling<sup>21</sup> between monomer IDT and DPP. All starting materials, reagents, and solvents were carefully purified, and all procedures were performed under an air-free environment. The structure of the polymer was confirmed by <sup>1</sup>H NMR spectroscopy and elemental analysis. PIDT-DPP has good solubility in common organic solvents such as THF, toluene, and chloro-

benzene, even in cold chloroform. It can be readily processed to form smooth and pinhole-free films on spin-coating.

### Thermal Analysis

The thermal properties of the polymer were determined by TGA and DSC under nitrogen. PIDT-DPP has good thermal stability with onset decomposition temperatures with 5% weight loss at 415 °C, as shown in Figure 1. When investigating the thermal behavior of the polymer using DSC, we observed no clear thermal transitions in the temperature range from 0 to 300 °C.



**SCHEME 3** Synthetic route of the copolymer. (i) Pd(dba)<sub>3</sub>, P(*o*-Tol)<sub>3</sub>, PhCl, 140 °C, 72 h.

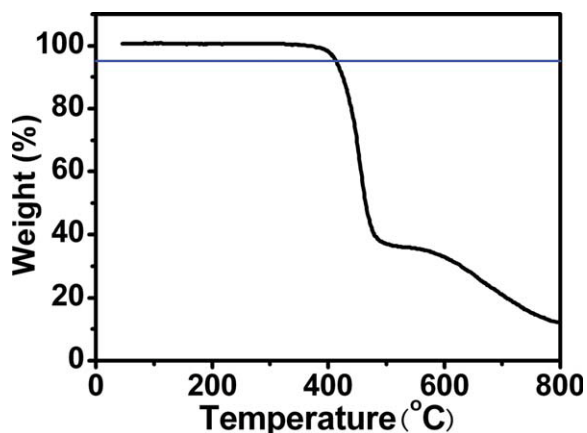


**FIGURE 1** TGA plot of the polymer with a heating rate of 10 °C/min under an inert atmosphere.

### Optical Properties

Figure 2 shows the absorption spectra of the polymer in chloroform solution and solid film on a quartz plate. In chloroform solution, the polymer exhibited a broad absorption from 350 to 850 nm. In solid film, the absorption spectrum was even expanded to 900 nm with an enhanced shoulder at 675 nm. The absorption peak of PIDT-DPP in solution and solid film are both centered at 735 nm. The optical band gap ( $E_g^{opt}$ ) determined from the onset of absorption of PIDT-DPP film was 1.37 eV. The small value of  $E_g$  of the copolymer is due to intramolecular charge transfer<sup>22-27</sup> between the IDT moieties and DPP unit. A small value of  $E_g$  should improve light harvesting and, therefore, could enhance the photocurrent of the PSCs.

### Electrochemical Properties

Cyclic voltammetry has been used and considered as an effective tool in investigating electrochemical properties of conjugated oligomers and polymers.<sup>28</sup> From the onset oxidation and reduction potentials in the cyclic voltammogram, energy levels of the highest occupied molecular orbital (HOMO) and

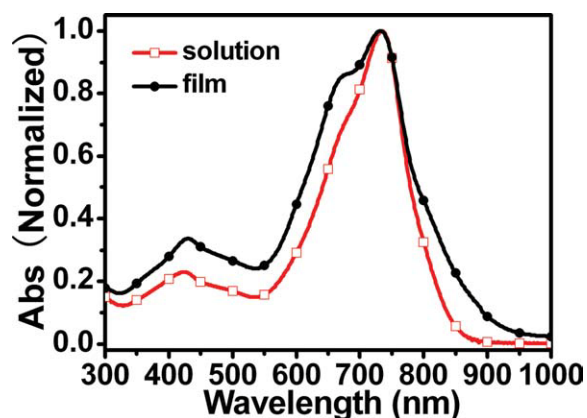


**FIGURE 2** Normalized absorption spectra of the PIDT-DPP in chloroform solution and solid film on a quartz plate.

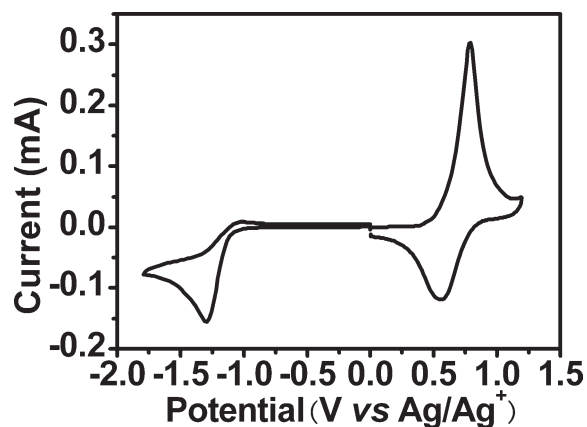


**FIGURE 3** Cyclic voltammogram of the polymer film on Pt electrode in 0.1 mol/L Bu<sub>4</sub>NPF<sub>6</sub>, CH<sub>3</sub>CN solution with a scan rate of 100 mV/s.

the lowest unoccupied molecular orbital (LUMO) energy levels can be readily estimated, which correspond to ionization potential and electron affinity, respectively.<sup>2</sup>

Cyclic voltammogram of the polymer film is shown in Figure 3. The onset oxidation potential ( $E_{ox}$ ) and onset reduction potential ( $E_{red}$ ) of PIDT-DPP are 0.61 V versus Ag/Ag<sup>+</sup> and -0.98 V versus Ag/Ag<sup>+</sup>, respectively. The HOMO and LUMO energy levels of the polymer are calculated from the onset oxidation potential and the onset reduction potential according to the equations: HOMO = -e ( $E_{ox}$  + 4.71) (eV) and

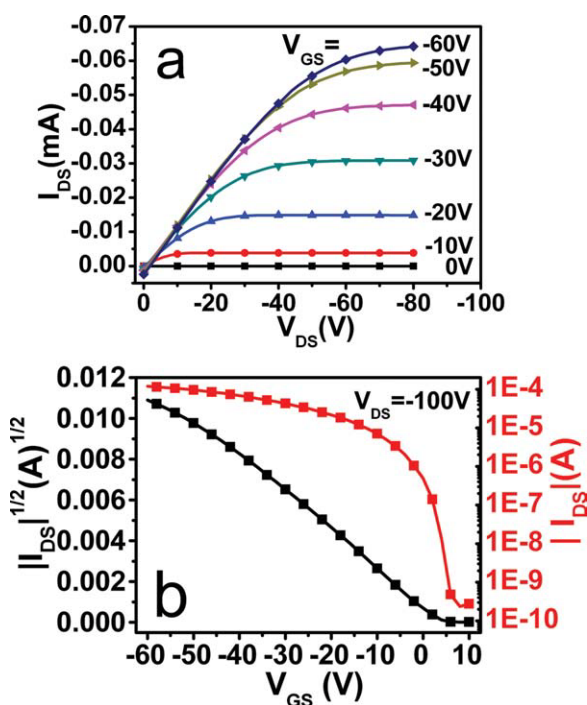


**FIGURE 4** (a) Output and (b) transfer characteristics of top-contact OFET using PIDT-DPP as the active layer (annealed at 80 °C).

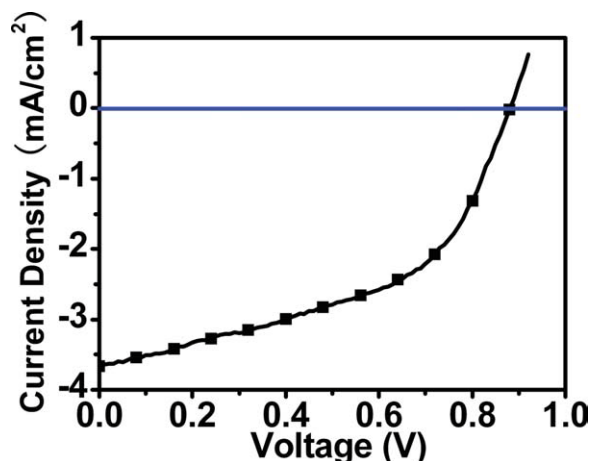
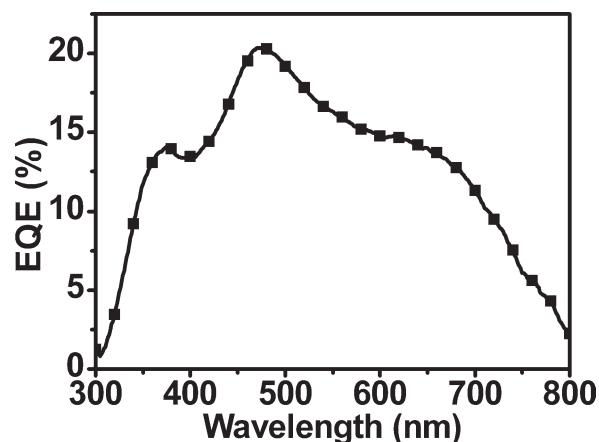
**TABLE 1** FET Properties of Devices with the PIDT–DPP Films Spin-Coated on OTS-Modified SiO<sub>2</sub>/Si Substrates

|                    | $\mu$ (cm <sup>2</sup> V <sup>-1</sup> s <sup>-1</sup> ) | $I_{on}/I_{off}$  | Threshold Voltage (V) |
|--------------------|--|-------------------|-----------------------|
| Without annealing  | 0.042  | $9.8 \times 10^5$ | -1                    |
| Annealed at 80 °C  | 0.065  | $4.6 \times 10^5$ | 3                     |
| Annealed at 100 °C | 0.023  | $2 \times 10^5$   | 0                     |

LUMO =  $-e(E_{red} + 4.71)$  (eV).<sup>29,30</sup> The calculated HOMO and LUMO energy levels of the polymer are  $-5.32$  eV and  $-3.73$  eV, respectively. It is obvious that the optical and electrochemical bandgaps of polymer are not similar (1.37 vs. 1.59 eV). The deviation could be attributed to the fact that the values obtained for the frontier-orbital energy levels cannot be taken as absolute due to strongly aggregate tendency of the polymer in solid state; therefore, the choice of solvents and concentration of a spin-coated film can greatly affect the morphology of polymer and as a result can affect UV-vis measurements. Compared to the HOMO of P3HT ( $-4.76$  eV<sup>30</sup>), that of PIDT–DPP is about 0.5 eV lower, which means a higher  $V_{oc}$  could be expected, because  $V_{oc}$  is linearly correlated with the difference of the HOMO of the donor and the LUMO of the acceptor.<sup>24,31</sup>

#### Field-Effect Transistor Properties of the Polymer

Figure 4 shows the typical output and transfer curves of the OFET device with PIDT–DPP as an active layer. The device performances of the polymer are summarized in Table 1. The output behavior closely followed the metal-oxide semiconductor FET gradual-channel model with very good saturation [Fig. 4(a)]. The transfer characteristics of PIDT–DPP-based devices showed a low drain current at zero gate voltage [Fig. 4(b)]. Without annealing, the OFET showed a hole mobility of  $0.042$  cm<sup>2</sup> V<sup>-1</sup> s<sup>-1</sup> in the saturation regime, together with an on/off ratio of  $9.8 \times 10^5$  when measured under an ambient conditions. Annealing the devices at 80 °C

**FIGURE 5** Current density–potential characteristic of PSC based on PIDT–DPP:PC<sub>71</sub>BM (1:1 w/w) under illumination of AM 1.5G, 100 mW/cm<sup>2</sup>.**FIGURE 6** The EQE spectrum of the device based on PIDT–DPP/PC<sub>71</sub>BM (1:1 w/w).

for 2.5 min led to improved hole mobility of up to  $0.065$  cm<sup>2</sup> V<sup>-1</sup> s<sup>-1</sup> with an on/off ratio of  $4.6 \times 10^5$  and a threshold voltage of 3 V.

#### Photovoltaic Properties of the Polymer

Another motivation of the design and synthesis of the polymer PIDT–DPP is to look for a novel alternating D–A copolymer based on fused ladder alkyl substituted IDT for the application in PSCs. We fabricate the PSCs with the structure of ITO/PEDOT: PSS/polymer:PC<sub>71</sub>BM (1:1 w/w)/Ca/Al, where the polymer (PIDT–DPP) was used as the electron donor and PC<sub>71</sub>BM was used as the electron acceptor. Figure 5 shows the  $I$  versus  $V$  curve of the PSCs under the illumination of AM 1.5 and 100 mW/cm<sup>2</sup>. It showed a PCE of 1.76% with an open circuit voltage ( $V_{oc}$ ) of 0.88 V, a short circuit current density ( $J_{sc}$ ) of 3.66 mA/cm<sup>2</sup>, and a fill factor of 0.54. The high value of  $V_{oc}$  of the device based on PIDT–DPP is benefited from the low HOMO energy level of the polymer. The external quantum efficiency (EQE) spectrum of the device are shown in Figure 6. The device exhibited photoresponse covering from 300 to 800 nm with an EQE value of more than 10% in the region between 340 and 715 nm. The  $J_{sc}$  calculated from the EQE curves are 3.63 mA/cm<sup>2</sup> for the device, showing a mismatched factor less than 1% compared with those values measured under AM 1.5G illumination. The relatively lower EQE value of the PSC based on PIDT–DPP could be due to low LUMO energy level ( $-3.73$  eV) of the polymer, which is only 0.18 eV higher than that ( $-3.91$  eV)<sup>32,33</sup> of PC<sub>71</sub>BM. If we can move the LUMO level of the polymer up-shifted and then combine the broad absorption spectrum, high charge carrier mobility, and deep HOMO, the polymer could become a promising high efficiency donor material in PSCs.

#### CONCLUSIONS

We designed and synthesized a novel D–A copolymer, PIDT–DPP, based on alkyl substituted IDT as a new donor unit and DPP as acceptor unit. The polymer possesses good thermal stability ( $T_d > 415$  °C) and exhibits a broad absorption spectrum from 350 to 900 nm with a narrow band gap of

1.37 eV. The solution-processed OFET with PIDT-DPP as the active layer showed a hole mobility of  $0.042 \text{ cm}^2 \text{ V}^{-1} \text{ s}^{-1}$  together with an on/off ratio of  $9.8 \times 10^5$ . Annealing the devices at  $80 \text{ }^\circ\text{C}$  greatly increased the hole mobility up to  $0.065 \text{ cm}^2 \text{ V}^{-1} \text{ s}^{-1}$  with an on/off ratio of  $4.6 \times 10^5$ . The PSC fabricated from the blend of PIDT-DPP and PC<sub>71</sub>BM exhibited PCEs of 1.76% with a high  $V_{oc}$  of 0.88 V, which is benefitted from the deep HOMO levels ( $-5.32 \text{ eV}$ ) of the polymer. These results indicate that this kind D-A copolymer based on the alkyl substituted IDT may become a promising active material for field-effect transistor, PSCs and other organic electronic devices.

This work was supported by NSFC (Nos. 20874106 and 21021091), The Ministry of Science and Technology of China and Chinese Academy of Sciences.

## REFERENCES AND NOTES

- Service, R. F. *Science* **2011**, *332*, 293.
- Wang, X. C.; Wang, H. Q.; Yang, Y.; He, Y. J.; Zhang, L.; Li, Y. F.; Li, X. Y. *Macromolecules* **2010**, *43*, 709–715.
- Burroughes, J. H.; Bradley, D. D. C.; Brown, A. B.; Marks, R. N.; Mackay, K.; Friend, R. H.; Bum, P. L.; Holmes, A. B. *Nature (London)* **1990**, *347*, 539–541.
- Allard, S.; Forster, M.; Souharce, B.; Thiem, H.; Scherf, U. *Angew. Chem. Int. Ed.* **2008**, *47*, 4070–4098.
- Li, Y. F.; Zou, Y. P. *Adv. Mater.* **2008**, *20*, 2952–2958.
- Wang, M.; Hu, X. W.; Liu, P.; Li, W.; Gong, X.; Huang, F.; Cao, Y. *J. Am. Chem. Soc.* **2011**, *133*, 9638–9641.
- Huo, L. J.; Guo, X.; Zhang, S. Q.; Li, Y. F.; Hou, J. H. *Macromolecules* **2011**, *44*, 4035–4037.
- Chen, H. Y.; Hou, J. H.; Zhang, S. Q.; Liang, Y. Y.; Yang, G. W.; Yang, Y.; Yu, L. P.; Wu, Y.; Li, G. *Nat. Photon.* **2009**, *3*, 649–653.
- Chen, X. W.; Liao, J. L.; Liang, Y. M.; Ahmed, M. O.; Tseng, H. E.; Chen, S. A. *J. Am. Chem. Soc.* **2003**, *125*, 636–637.
- Guo, Y. L.; Yu, G.; Liu, Y. Q. *Adv. Mater.* **2010**, *22*, 4427–4447.
- Zhang, W. M.; Scott, E.; Watkins, J. S.; Gysel, R.; McGehee, M.; Salleo, A.; Kirkpatrick, J.; Ashraf, S.; Anthopoulos, T.; Heeney, M.; McCulloch, I. *J. Am. Chem. Soc.* **2010**, *132*, 11437–11439.
- Chen, C. P.; Chan, S. H.; Chao, T. C.; Ting, C.; Ko, B. T. *J. Am. Chem. Soc.* **2008**, *130*, 12828–12833.
- Yu, C. Y.; Chen, C. P.; Chan, S. H.; Hwang, G. W.; Ting, C. *Chem. Mater.* **2009**, *21*, 3262–3269.
- Zhang, Y.; Zou, J. Y.; Yip, H. L.; Chen, K. S.; Zeigler, D. F.; Sun, Y.; Jen, A. K. Y. *Chem. Mater.* **2011**, *23*, 2289–2291.
- Chen, Y. C.; Yu, C. Y.; Fan, Y. L.; Hung, L. I.; Chen, C. P.; Ting, C. *Chem. Commun.* **2010**, *46*, 6503–6505.
- Bronstein, H.; Chen, Z. Y.; Ashraf, R. S.; Zhang, W. M.; Du, J. P.; Durrant, J. R.; Tuladhar, P. S.; Song, K.; Watkins, S. E.; Wienk, Y. G. M. M.; Janssen, R. A. J.; Anthopoulos, T.; Sirringhaus, H.; Heeney, M.; McCulloch, I. *J. Am. Chem. Soc.* **2011**, *133*, 3272–3275.
- Wienk, M. M.; Turbiez, M.; Gilot, J.; Janssen, R. A. J. *Adv. Mater.* **2008**, *20*, 2556–2560.
- Bijleveld, J. C.; Zoombelt, A. P.; Mathijssen, S. G. J.; Wienk, M. M.; Turbiez, M.; de Leeuw, D. M.; Janssen, R. A. J. *J. Am. Chem. Soc.* **2009**, *131*, 16616–16617.
- Ashraf, R. S.; Chen, Z.; Leem, D. S.; Bronstein, H.; Zhang, W.; Schroeder, B.; Geerts, Y.; Smith, J.; Watkins, S.; Anthopoulos, T. D.; Sirringhaus, H.; de Mello, J. C.; Heeney, M.; McCulloch, I. *Chem. Mater.* **2011**, *23*, 768–770.
- Woo, C. H.; Beaujuge, P. M.; Holcombe, T. W.; Lee, O. P.; Frechet, J. M. J. *J. Am. Chem. Soc.* **2010**, *132*, 15547–15549.
- Bao, Z. N.; Chan, W. K.; Yu, L. P. *J. Am. Chem. Soc.* **1995**, *117*, 12426–12435.
- Ego, C.; Marsitzky, D.; Becker, S.; Zhang, J.; Grimsdale, A. C.; Mullen, K.; MacKenzie, J. D.; Silva, C.; Friend, R. H. *J. Am. Chem. Soc.* **2003**, *125*, 437–443.
- Tu, G. L.; Mei, C. Y.; Zhou, Q. G.; Cheng, Y. X.; Geng, Y. H.; Wang, L. X.; Ma, D. G.; Jing, X. B.; Wang, F. S. *Adv. Funct. Mater.* **2006**, *16*, 101–106.
- Scharber, M. C.; Muhlbacher, D.; Koppe, M.; Denk, P.; Wal-fauf, C.; Heeger, A. J.; Brabec, C. J. *Adv. Mater.* **2006**, *18*, 789–794.
- Coakley, K. M.; McGehee, M. D. *Chem. Mater.* **2004**, *16*, 4533–4542.
- Li, G.; Shrotriya, V.; Huang, J.; Yao, Y.; Moriarty, T.; Emery, K.; Yang, Y. *Nat. Mater.* **2005**, *4*, 864–868.
- Peet, J.; Kim, J. Y.; Coates, N. E.; Ma, W. L.; Moses, D.; Heeger, A. J.; Bazan, G. C. *Nat. Mater.* **2007**, *6*, 497–500.
- Li, Y. F.; Cao, Y.; Gao, J.; Wang, D. L.; Yu, G.; Heeger, A. J. *Synth. Met.* **1999**, *99*, 243–248.
- Sun, Q. J.; Wang, H. Q.; Yang, C. H.; Li, Y. F. *J. Mater. Chem.* **2003**, *13*, 800–806.
- Hou, J. H.; Tan, Z. A.; Yan, Y.; He, Y. J.; Yang, C. H.; Li, Y. F. *J. Am. Chem. Soc.* **2006**, *128*, 4911–4916.
- Huo, L. J.; Hou, J. H.; Zhang, S. Q.; Chen, H. Y.; Yang, Y. *Angew. Chem. Int. Ed.* **2010**, *49*, 1500–1503.
- He, Y. J.; Li, Y. F. *Phys. Chem. Chem. Phys.* **2011**, *13*, 1970–1983.
- He, Y. J.; Zhao, G. J.; Peng, B.; Li, Y. F. *Adv. Funct. Mater.* **2010**, *20*, 3383–3389.